Earth, Planets and Space

FULL PAPER Open Access

Multi-method constraints on the age and timescale of silicic small-volume eruptions of Puketerata Volcanic Complex, Taupō Volcanic Zone, New Zealand

Szabolcs Kósik[1*], Takeshi Hasegawa[2], Martin Danišík[3], Károly Németh[4,5], Makoto Okada[2], Bjarne Friedrichs[6,7] and Axel K. Schmitt[6]

Abstract

Accurate dating of young eruptions from explosive volcanoes is essential for forecasting future eruptions and for defining the hazardscape of volcanic fields. However, precise dating of Quaternary eruptions is often challenging due to limited number of applicable dating methods or lack of datable eruptive phases. Moreover, small volume eruptions (e.g., monogenetic type), despite their significance on regional scale, have traditionally deserved less attention than their large volume counterparts. Puketerata is a maar-lava dome complex in the central Taupō Volcanic Zone (New Zealand), encompassing mafic and silicic phreatomagmatic eruptions with well-preserved pyroclastic deposits sourced from closely spaced vents. Its most recent activity is estimated to ca. 16 ka based on medial and distal stratigraphic surveys. Here, we carried out two independent age determinations and an additional paleomagnetic analysis on the volcanic succession of the Puketerata maar-lava dome complex with an aim to unravel the timing of volcanic activity. Combined U-Th disequilibrium and (U-Th)/He dating of zircon from two lava domes yielded eruption ages of 11.3 ± 2.6 ka and 11.3 ± 1.7 ka, which are concordant with the radiocarbon ages of 11.3–11.7 ka obtained on charcoal from the base of the pyroclastic sequence. Paleomagnetic data on the lavas from the two lava domes suggest at least ~ 100 years difference between their emplacements. Our geochronological results and new stratigraphic observations suggest that the volcanic/magmatic history of the Puketerata is complex with multiple eruptions within a small, confined area, where the most recent eruptions occurred only at ca. 11.5 ka, which is significantly younger than previously thought. This provides an additional datum for volcanic hazards assessment and stratigraphic correlations in New Zealand.

Keywords Lava dome, Tephra stratigraphy, Paleomagnetic dating;, Radiocarbon dating, U-Th disequilibrium, (U-Th)/He, Pyroclastic density currents, Maar, Phreatomagmatism, Taupō Volcanic Zone

*Correspondence:
Szabolcs Kósik
szabolcs.kosik@gmail.com
Full list of author information is available at the end of the article

Graphical Abstract

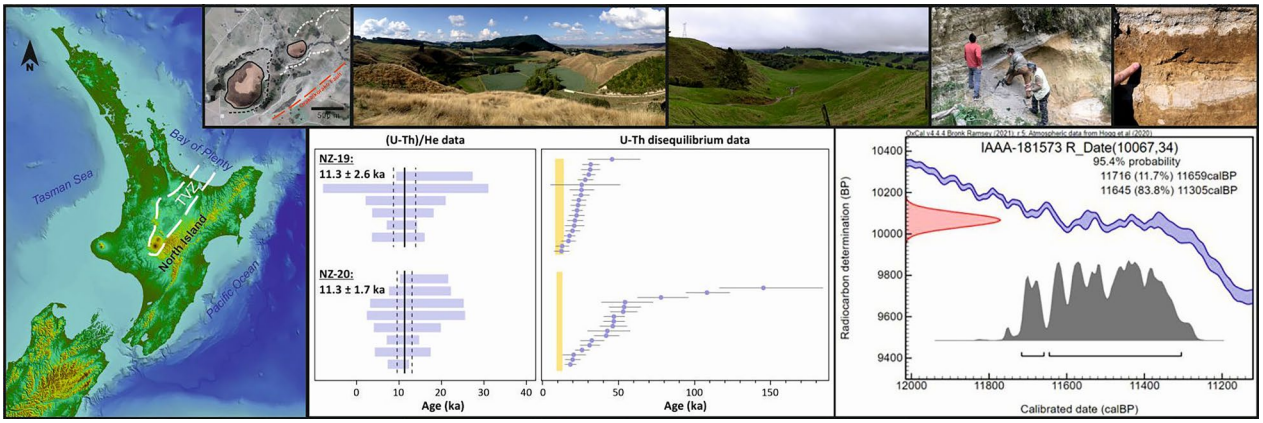

Introduction

Small-volume volcanism is most frequently associated with volcanic fields (e.g., Németh 2010). However, small-volume eruptions have also been reported from large silicic caldera systems, such as the central Taupō Volcanic Zone (TVZ), New Zealand, where they are spatially and temporally dispersed among the much larger volume caldera forming eruptions (Kósik et al. 2020; Sourisseau et al. 2020). Small-volume eruptions are generally fed by small-volume magma batches, their duration is rather short (hours to months) and they create a new vent and form simple types of volcanoes such as scoria cones or lava domes (Németh 2010; Smith and Németh 2017). In many cases, the architecture of these volcanoes can be complex due to the changes in eruption style that are affected by the variability of the eruption site environment during magma venting (e.g., Valentine and Gregg 2008; Németh 2010; Kurszlaukis and Fulop 2013; Németh and Kereszturi 2015; Smith and Németh 2017; Kósik et al. 2021, 2022). Dating of eruption phases of small-volume eruptions is often challenging due to the lack of sufficiently accurate and precise dating techniques (e.g., Fulop and Kurszlaukis 2014; Chako-Tchamabé et al. 2016).

The Puketerata (or Puketarata) Volcanic Complex (PVC) is a complex small-volume volcano, comprising two silicic lava domes and several coalesced maar craters along a ≥ 2.5 km long fissure vent in the central TVZ (Kósik et al. 2019). The significance of the PVC lies in the intact nature of its pyroclastic successions (e.g., well preserved tuff rings) particularly at proximal and medial locations, which has enabled characterisation of the complex nature of a rhyolitic explosive to effusive small-volume eruption (Brooker et al. 1993; Kósik et al. 2019). However, the timing of this eruption is disputable.

Inferring from the well-preserved nature of the pyroclastic deposits and morphology of the ejecta ring that surrounds the larger dome, Lloyd (1972) suggested that the eruptions of PVC are significantly younger than other nearby small eruptions. The hitherto accepted age of ca. 16 ka for the PVC activity (e.g., Leonard et al. 2010) has been derived from early stratigraphic observations (Vucetich and Pullar 1969, 1973; Lloyd 1972; Topping 1973; Topping and Kohn 1973; Lowe 1988). However, many of the observations were made at locations that were shown unlikely to receive tephra fall from the PVC eruption based on isopach maps (Lloyd 1972; Brooker et al. 1993) and the characterisation of explosive activity (Kósik et al. 2019). No absolute dating has been attempted on the PVC so far.

In this study, we aim to address this issue and attempt to date the PVC volcanic activity by employing a range of dating methods. These include combined U-Th disequilibrium and (U-Th)/He dating of zircon (a.k.a. zircon double-dating or ZDD; Schmitt et al. 2006; Danišík et al. 2017) applied to samples from two lava domes, and also radiocarbon (^{14}C) dating of charcoal extracted from underlying sequences. In addition, to further investigate the complex nature of the activity with common changes of eruption styles documented for PVC earlier by Brooker et al. (1993) and Kósik et al. (2019), we apply a novel methodology based on the difference of paleomagnetic attributes of the lavas from the two lava domes and also present stratigraphic and sedimentological observations for a newly discovered exposure displaying the PVC sequence. Our findings not only put into question the currently accepted age and stratigraphic position of Puketerata tephra, but also suggest that the time gap between the emplacement of the two lava domes was

sufficiently long to subdivide the activity to two separate volcanic events.

Geological setting

The TVZ is a rifting arc located at the southern end of the Tonga-Kermadec arc and has been forming for the past 2 Myrs as a result of the oblique subduction of the Pacific plate underneath the Indo-Australian plate and the associated back-arc extension (e.g., Cole 1990; Davey et al. 1995; Wilson et al. 1995; Acocella et al. 2003; Wallace et al. 2004; Spinks et al. 2005; Reyners 2013). The northern (Bay of Plenty) and the southern parts (Tongariro Volcanic Centre) of the TVZ are characterised by mostly andesitic volcanism, while the central TVZ is dominated by rhyolitic volcanism that has formed seven calderas/caldera complexes with hundreds of lava domes over the past 350 kyrs (Wilson et al. 1995; Spinks et al. 2005; Kósik et al. 2020). The PVC is in the rhyolitic central segment of the TVZ within the Whakamaru caldera formed at ca. 350 ka (Brown et al. 1998; Downs et al. 2014). Post-caldera volcanism was mostly characterised by lava dome emplacement and associated explosive activity occurring irregularly after 305 ka (Leonard et al. 2010). The loci of dome forming eruptions are two linear vent zones in the central part of the caldera (identified as Maroa Volcanic Centre—MVC; Leonard 2003; Leonard et al. 2010), similarly to the present settings of Okataina Volcanic Centre (Nairn 2002).

The PVC represents the youngest dome forming event at the southern margin of MVC (Leonard 2003) with well-preserved pyroclastic density current (PDC)-dominated successions (Brooker et al. 1993; Kósik et al. 2019). The PVC formed on a fault-bounded, gently incised ignimbrite-dominated topography (Fig. 1b). The proximal and medial sequences of the PVC are usually underlain by a 1–2 m thick sandy soil and loess (Vucetich and Pullar 1969), which were deposited on the erosion surface of multiple ignimbrite sheets (e.g., Orakonui Formation (254 ka) and Oruanui Formation (25.4 ka); Leonard 2010) and pyroclastic sequences of the undated Te Hukui Basalt (Kósik et al. 2017). The eruptive vents of the PVC were formed along a lineament parallel to the nearby NE-trending Orakeikorako Fault. At the examined proximal and medial exposures of Puketerata the only collectable overlaying tephra is associated with the 1.8 ka Taupo Pumice Formation (Hogg et al. 2012), whereas the stratigraphy proposed by Vucetich and Pullar (1969, 1973) could not been confirmed (Kósik et al. 2019).

The Pukaterata activity has been divided into two phases based on the volcanic architecture (Fig. 1c). The initial phase has created multiple coalesced maar craters in linear arrangement along the NE-SW trending Orakeikorako Fault. The second phase was manifested by lava effusion from two separate vents forming two lava domes and phreatomagmatic to Vulcanian activity from the vents of the larger dome located at the SW end of the fissure (Brooker et al. 1993; Kósik et al. 2019). The smaller dome is located in a lower topographic position and is partly covered by a thick layer of tephra associated with the activity of the larger dome (Kósik et al. 2019). This indicates that the vents of the larger dome remained active after the emplacement of the smaller dome. The morphology of the two domes and the chemical composition and petrography of their rhyolites are slightly different (Kósik et al. 2019). The smaller lava dome has a simple shape with steep sides indicating high yield strength at the time of extrusion, whereas the larger lava dome is more irregular in shape indicating multiple growth and destruction cycles during its emplacement (Kósik et al. 2019). Major element geochemistry shows lower SiO_2 and higher TiO_2, FeO* and MgO for the rhyolite of the larger dome beyond standard deviations (Supplementary table 1).

Zircon U-Th disequilibrium model ages reported for Puketerata rocks by Wilson and Charlier (2009) range between 151 ± 17 and 14.8 ± 3.1 ka and indicate a peak crystallization period at ca. 25 ka. The youngest zircon crystallization age is within analytical error of the stratigraphically inferred eruption age (ca. 16 ka), but U-Th ages are crystallization ages that only provide a maximum limit for the eruption age.

Samples and methodology

Radiocarbon dating

With the aim to unfold the eruptive history of Puketerata, one sample of charcoal for ^{14}C dating was collected from the base of the Puketerata pyroclastic succession exposed in the gully between the ejecta ring east of the larger dome and the Orakeikorako Fault (locality 3–23 in Figs. 1c and 2). The sample was dated using Accelerator Mass Spectrometry (AMS) at the Institute of Accelerator Analysis Ltd. (Japan) equipped with a 3 MV Tandem Accelerator system (NEC Pellerton, 9SDH-2). Prior to analysis, the trimmed sample block was dispersed in pure water by ultrasonic washer and sieved to remove contamination. The dried sample was purified by routine acid–alkali–acid (AAA) treatments. The pre-treated sample was oxidized by heating to generate CO_2 and the CO_2 was cryogenically liberated and purified in a vacuum line. The derived CO_2 was reduced catalytically to graphite on Fe-powder. The carbon in the graphite was ionized, and the ionized carbon was accelerated and measured via AMS systems to detect the ^{14}C atoms, the ratio of $^{13}C/^{12}C$ and $^{14}C/^{12}C$ atom with NIST oxalic acid (HOxII) as the standard reference material. The AMS ^{14}C value was corrected for isotopic fractionation and calibrated

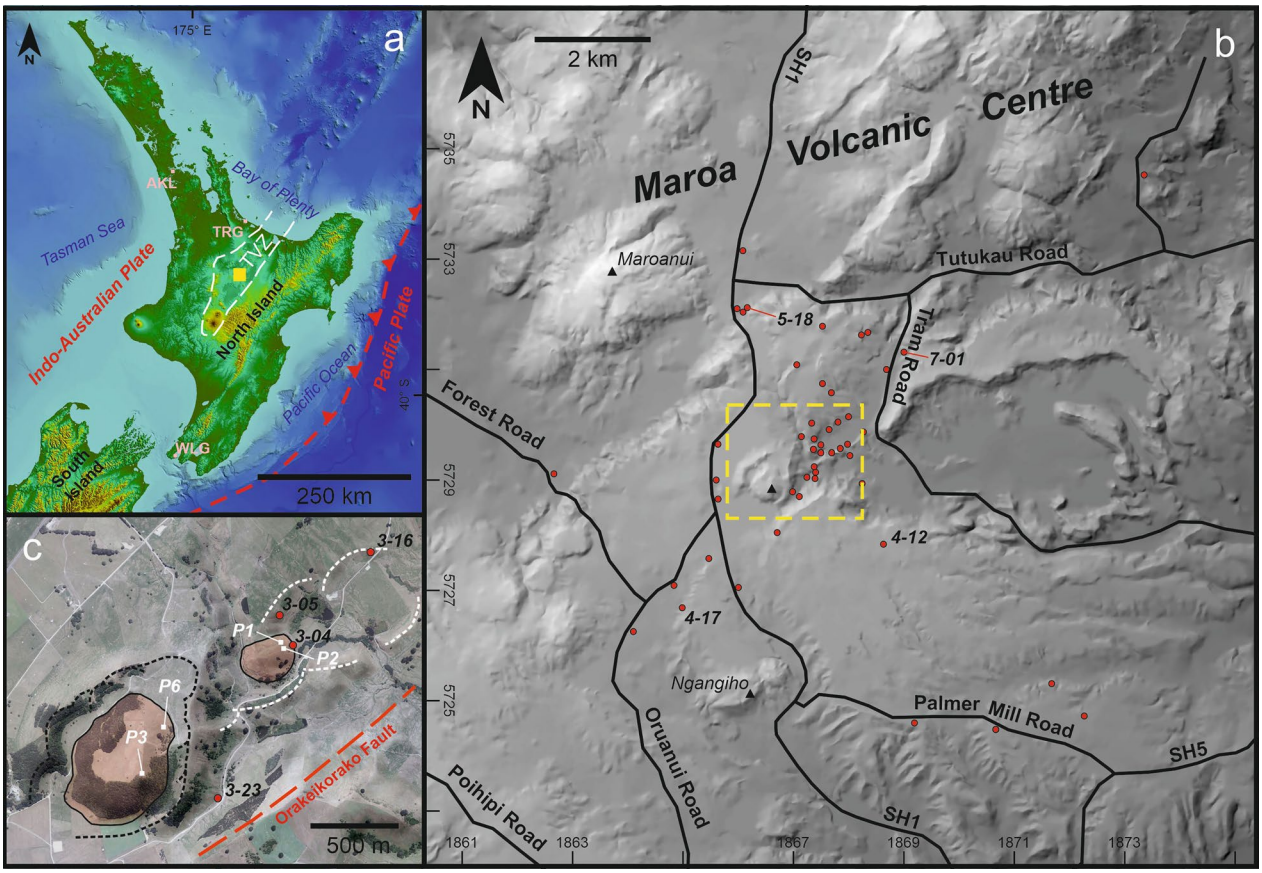

Fig. 1 **a** Digital elevation model showing the geographic location of the Taupō Volcanic Zone (TVZ) and the study area within the New Zealand North Island and its relative position to the plate boundary. Background bathymetric information is derived from the 250 m resolution gridded bathymetric data from National Institute of Water and Atmospheric Research (NIWA) 2016. *AKL* Auckland, *TRG* Tauranga, *WLG* Wellington. **b** Topography of the broader area of Puketerata maar—lava dome complex with main roads and investigated medial to distal exposures of Puketerata deposits (red circles). Yellow dashed rectangle indicates the extent of inset c. The coordinate system is given in New Zealand Transverse Mercator 2000 (NZTM2000) projection. **c** Volcanic architecture of the PVC: red shaded areas—lava domes; black dashed line—rim of the tuff ring surrounding the larger lava dome; white dashed lines—rims of maar craters; white squares with IDs—the sites for paleomagnetic sampling. Hillshade raster for **b**, **c** was derived from the 8 m NZ DEM (LINZ—Land Information New Zealand, 2012, https://data.linz.govt.nz/)

to calendar years using the OxCal 4.3.2 program (Bronk Ramsey 2017) with the SHCal20 calibration curve (Hogg et al. 2020).

Zircon double-dating

Two samples (NZ-19 and NZ-20) of the fragments from lava domes (localities 3–04 and 3–16, respectively, in Fig. 1c) were dated by zircon double-dating (ZDD) to constrain zircon crystallization and eruption history. Sample NZ-19 (locality 3–04 in Fig. 1c) was collected from the edge of the small lava dome; sample NZ-20 (locality 3–16 in Fig. 1c) was collected from the pyroclastic deposits emplaced during the formation of the large lava dome. The samples were split into 3–5 cm fragments some of which were submitted to Labwest Minerals Analysis Pty Ltd. (Perth, Australia) for trace element analysis by solution ICP-MS (Perking Elmer 296 NexION 300Q) to determine the whole rock Th/U values that are required for ZDD age calculation (Schmitt 2011; Danišík et al. 2017). The remaining rock fragments were separated for zircon following a standard workflow for heavy mineral separation at the John de Laeter Centre, Curtin University, Australia. The procedure included disaggregation by SelFrag, magnetic and heavy liquid separation, hand-picking under a binocular microscope and rinsing in cold 40% HF to remove adhering glass (Danišík et al. 2020).

Zircon crystals were submitted to the Heidelberg Ion-Probe (HIP) Laboratory at the Institute of Geosciences, Heidelberg University (Germany), for U-Th disequilibrium analysis to constrain crystallization ages that are required for the disequilibrium correction of (U-Th)/He dates (Farley et al. 2002; Schmitt et al. 2006, 2010). Zircon crystals were embedded in indium (In) metal with

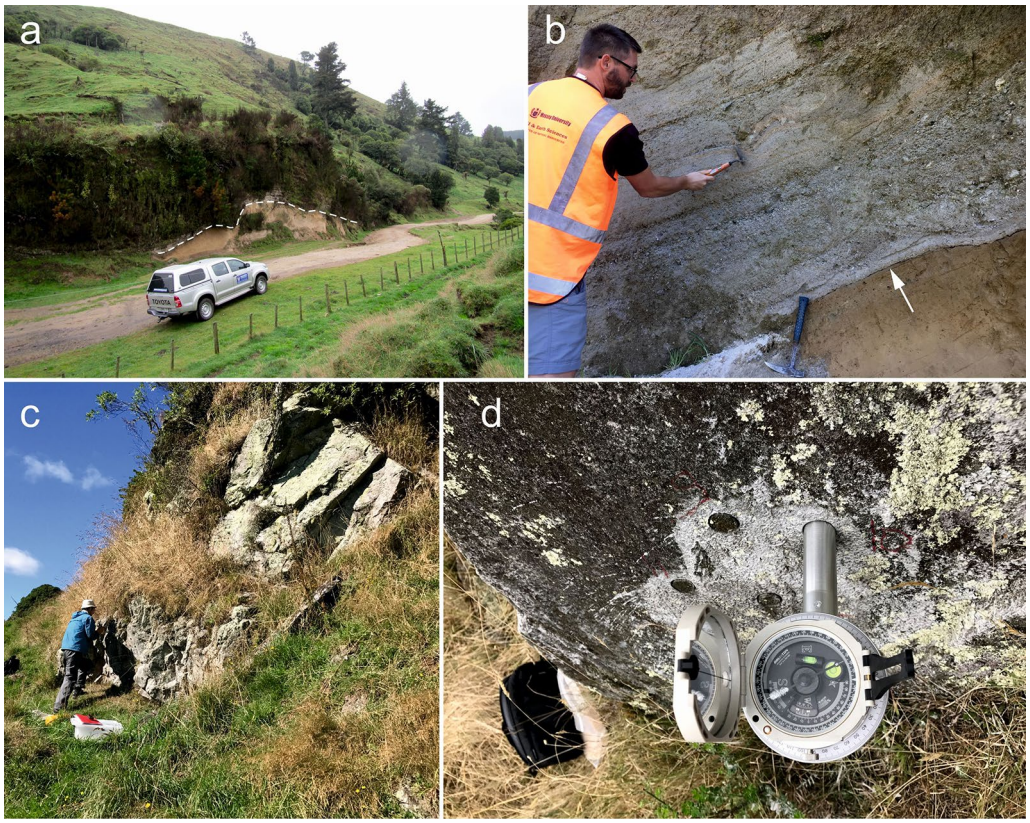

Fig. 2 Geological context of charcoal and paleomagnetic sampling; **a** Locality 3–23 (Fig. 1c) with the base of the main pyroclastic sequence. White dashed line represents the contact between pre-Puketerata paleosol and Puketerata pyroclastic deposits. **b** Close-up view to the base of the pyroclastic sequence at locality 3–23 with the dark strata with charcoal content indicated by white arrow. **c** Paleomagnetic sampling at locality P6 (Fig. 1c) from the larger lava dome. **d** Paleomagnetic sampling at locality P2 from the smaller lava dome

unpolished crystal faces exposed at the surface, levelled, and coated with a conductive layer of gold. Crystal rims were dated by U-Th disequilibrium methods with a CAMECA IMS 1280-HR (SIMS) following the protocols for dynamic multi-collection analysis described by Schmitt et al. (2017) and Friedrichs et al. (2020).

After the SIMS analysis, zircon crystals were plucked out of the In based on their size, shape and crystallization age in the JdLC Western Australia ThermoCHronology (WATCH) Facility (Curtin University), photographed, measured for physical dimensions, and dated by conventional single grain (U-Th)/He dating procedures as detailed in Danišík et al. (2020). ^{4}He was analyzed by isotope dilution on an Alphachron II instrument; U and Th were analyzed by isotope dilution on an Element XR™ High Resolution ICP-MS. The total analytical uncertainty (TAU) was calculated as a square root of sum of squares of uncertainty on He and weighted uncertainties on U, Th, and He measurements. The raw zircon (U-Th)/He dates were corrected for alpha ejection (Ft correction) after Farley et al. (1996), whereby homogenous distributions of U and Th were assumed for the crystals. The accuracy of the zircon (U-Th)/He dating procedure was monitored by replicate analyses of internal standard Fish Canyon Tuff zircon where crystals measured over the course of this study yielded a mean (U-Th)/He age of 28.4 ± 1.7 Ma (95% conf. int.; $n = 3$; Supplementary table 1), in excellent agreement with the reference (U-Th)/He age of 28.3 ± 1.3 Ma (Reiners 2005). The Ft-corrected (U-Th)/He dates were corrected for U-series disequilibrium and pre-eruptive crystal residence time (Farley et al. 2002) using MCHeCalc software (Schmitt et al. 2010). The D_{230} parameter (Farley et al. 2002) was calculated by dividing zircon Th/U values by whole-rock Th/U, and assuming secular equilibrium as indicated by published whole-rock data (Wilson and Charlier 2009). For the D_{231} parameter, defined analogous to D_{230}, a value of 3.3 was adopted based on an average of published Pa/U zircon-rhyolite melt partition coefficient values (Schmitt 2007, 2011; Sakata et al. 2017). Disequilibrium corrected (U-Th)/He dates were then used to calculate error-weighted mean values (with 95% confidence intervals), which are interpreted as the eruption age of each sample (termed ZDD eruption age).

Paleomagnetic sampling and sample preparation

Sampling for paleomagnetic analysis was conducted at two locations on the large dome (sites P3 and P6; Fig. 1c) and two locations on the small dome (sites P1 and P2; Fig. 1c). At each location, homogenous parts of stable (not deformed) outcrop of lava domes were identified, and from these six closely spaced and ≥ 5 cm long cores were drilled (Fig. 2). Prior to removal from the outcrop, the cores were oriented using a magnetic compass and inclinometer. The measured azimuth was corrected for the local declination of 21° East (ref: International Geomagnetic Reference Field (IGRF-13)).

Cores were cut into ~ 2 cm long specimens for paleomagnetic measurements. Natural remanent magnetization (NRM) was measured using AGICO JR6 spinner magnetometer prior to and following stepwise thermal demagnetization at up to a peak temperature of ~ 630 °C using a TD-48, ASC Scientific furnace at Ibaraki University, Japan. Characteristic remanent magnetizations (ChRM) were subsequently determined by principal component analysis (Kirschvink 1980). ChRM directions were selected from the most stable component towards the origin, and sample data selected if the maximum angular deviation (MAD) was less than 5° (Supplementary table 1). Unit mean directions and 95% confidence intervals were calculated from individual specimen ChRM directions.

Results

Radiocarbon age

The charcoal sample (3–23) yielded a carbon isotopic ratio ($\delta^{13}C$) of 26.10 ± 0.48‰ and a conventional ^{14}C age (Libby age) of 10.067 ± 0.034 ka BP (Supplementary table 1). This age corresponds to two calibrated (95.4% probability) age ranges of 11.305–11.645 and 11.659–11.716 cal ka BP (Fig. 3).

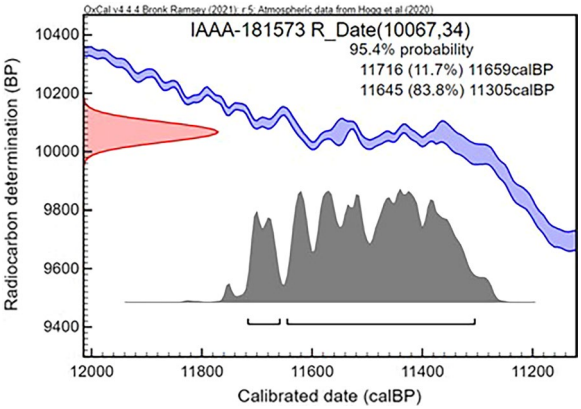

Fig. 3 Calibration of radiocarbon dating. Calendar age was calibrated by the OxCal v.4.4.4 program (Bronk Ramsey 2017) using the SHCal20 atmospheric curve (Hogg et al. 2020)

ZDD data

Analytical results of ZDD analysis are summarized in Fig. 4 and Table 1, and detailed in Supplementary table 1. Analyses of all crystal surfaces revealed ^{230}Th deficits, suggesting a crystallization age < < 350 ka for all 36 dated crystals. For sample NZ-19, U-Th model ages defined by zircon and whole rock compositions form a continuous, relatively narrow spectrum ranging from $12.5^{+5.2}_{-5.0}$ to $45.8^{+18.6}_{-15.9}$ ka (1σ; $n = 19$) (Fig. 4b). U-Th model ages for sample NZ-20 form a broader spectrum ranging from $18.4^{+3.8}_{-3.7}$ to $145.2^{+38.9}_{-28.6}$ ka (1σ; $n = 17$), but with the majority of the U-Th ages (i.e., 14 out of 17) overlapping with the U-Th model ages of sample NZ-19 (Fig. 4b). All U-Th model ages are consistently older or overlap within uncertainty with the corresponding ZDD eruption age.

Six and eight SIMS-dated zircon crystals from samples NZ-19 and NZ-20, respectively, were successfully dated by the (U-Th)/He method (Fig. 4a; Table 1). Alpha-ejection and disequilibrium corrected (U-Th)/He dates yield weighted mean values of 11.3 ± 2.6 ka (95% conf. interval; MSWD = 0.54; n = 6) for sample NZ-19 (locality 3–16 from pyroclastic deposit from large dome; Fig. 1c) and 11.3 ± 1.7 ka (95% conf. interval; MSWD = 0.76; n = 8) for sample NZ-20 (locality 3–04 from small dome; Fig. 1c). These values are interpreted as ZDD eruption ages for the dated samples; uncertainties reflect the low He content of these young crystals.

Paleomagnetic data

Almost all samples investigated by paleomagnetic analysis revealed a single stable component of magnetization converging toward the origin in the orthogonal vector plots during thermal demagnetizations (Fig. 5a). Although all samples were completely demagnetized by 600 °C, the samples from the large lava dome (PUK3 and 6) show abrupt decreases in remanence intensity between 500 and 600 °C, suggesting that the main magnetization components are carried by magnetite (unblocked between 500 and 580 °C). Samples from the smaller lava dome show relatively gentle decay curves indicative of the decomposition of (titano)maghemite and/or containing titano-magnetite. The ChRM directions from the smaller dome show easterly declination (10.7° to 23.5°), whereas the declination of those of the larger dome is close to true north. Consequently, the mean ChRM direction of small and large domes was calculated to be Dec = 15.3°/Inc = − 50.8° and Dec = 360°/Inc = − 54.8°, respectively. Both of the mean ChRM direction were well-defined with small (2.9° to 3.7°) alpha-95 values. Considering the

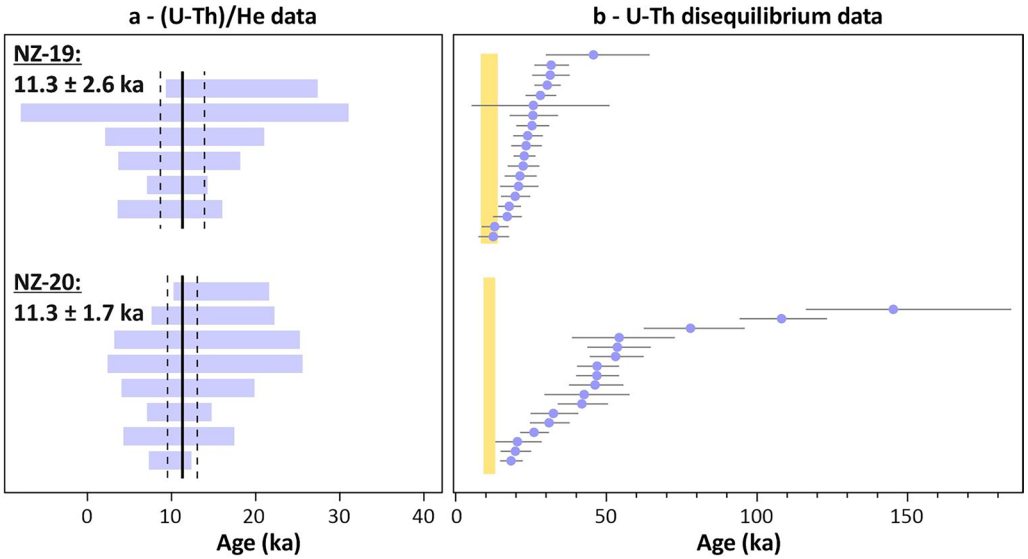

Fig. 4 **a** Rank order plots of Ft- and disequilibrium corrected zircon (U-Th)/He dates displayed as 2σ error bars. Eruption ages and corresponding 95% confidence intervals are listed as numerals and displayed as solid black vertical lines through each population and outer dashed black lines. **b** Rank order plots of U-Th disequilibrium model ages and 1σ error bars. Orange bars represent ZDD eruption ages that are displayed as 95% confidence intervals.

alpha-95, the two directions are distinct on the equal area projection (Fig. 5b).

New observations for stratigraphy and sedimentology

Since the earlier field work documented in Kósik et al. (2019), a new outcrop displaying the Puketerata sequence has been accessible due to earthworks in relation to forestry operation at locality 7–01 (Fig. 1b). Under the main Puketerata sequence, a ca. 10–12 cm discontinuous thick fine ash layer is found bracketed by paleosols (Fig. 6). In terms of appearance, it is very similar to medial/distal PDC deposits of the main Puketerata sequence. The newly found ash layer was divided to three units (a-c). The lowermost unit ("a" in Fig. 6) is an up to 1-cm-thick well-sorted medium ash layer with discontinuous appearance. Unit a is overlain by an up to 6-cm-thick light-cream-coloured, poorly sorted fine ash layer with accretionary lapilli up to 3 mm in diameter ("b' in Fig. 6). The topmost unit ("c" in Fig. 6) is a bioturbated fine ash with very similar grain size characteristics to unit b. This lower tephra layer is separated from the main Puketerata sequence by an organic matter rich paleosol having a thickness of 6 to 8 cm (Fig. 6).

According to the field assessment of sorting, "b" and "c" units of the lower tephra layer is interpreted to have a diluted PDC origin, whereas unit "a" is considered to being sourced from a fallout (Fig. 6). The abundance of accretionary lapilli supports the phreatomagmatic nature of the eruption that formed these deposits (Németh and Kósik 2020).

Discussion

Timing and duration of Puketerata activity

Based on the volcanic products and architecture of the volcanic structures, the PVC silicic activity can be subdivided into three phases—(1) initial maar forming activity, (2) emplacement of the small dome, and (3) emplacement of the larger dome and associated explosive activity forming a tuff ring (Fig. 1c). In earlier studies, the activity was considered as a one-off event with a relatively brief break in the explosive activity (Brooker et al. 1993; Kósik et al. 2019). In this study, age determination of the PVC activity was carried out by two independent radiometric methods that revealed indistinguishable results overlapping within analytical uncertainties that do not allow us to differentiate the proposed phases due to the limited precision of the dating methods applied. Extrusion of both lava domes is constrained by ZDD eruption ages to 11.3 ± 2.6 ka (pyroclastic deposit from the large lava dome) and 11.3 ± 1.7 ka (sample NZ-20; small lava dome). The deposition of the pyroclastic density currents at the base of the tuff ring, which is most likely associated with the effusive-explosive activity of phase 3, is constrained by ^{14}C dating to age ranges of 11.31–11.65 and 11.66–11.72 cal ka BP.

Nevertheless, there is a distinct paleomagnetic direction between the samples of the two domes, which suggests a considerable time break between their

Table 1 ZDD data summary

Sample code	^{232}Th (ng)	± (%)	^{238}U (ng)	± (%)	^{147}Sm (ng)	± (%)	^{4}He (ncc)	± (%)	TAU (%)	Th/U	Raw He age (ka)	±1σ (ka)	Ft	± (%)	Ft.-cor. He age (ka)	±1σ (ka)	U-Th (ka)	±1σ (ka)	D_{230}	Diseq.-cor He age (ka BP)	±1σ (ka)
NZ-19																					
NZ19-1	0.486	1.9	0.576	2.4	0.00026	1.4	0.0004	39.7	39.8	0.84	4.8	1.9	0.69	5	7.0	2.8	28.2	5.2	0.1698	11.6	4.8
NZ19-2	0.886	1.3	0.974	2.0	0.00026	1.9	0.0007	15.7	15.8	0.90	4.8	0.8	0.73	5	6.6	1.1	30.4	4.5	0.1831	10.7	1.8
NZ19-3	1.162	1.3	1.044	1.9	0.00010	1.9	0.0006	30.0	30.0	1.11	4.1	1.2	0.66	5	6.1	1.9	17.1	4.9	0.2240	9.8	3.2
NZ19-4	0.383	1.9	0.546	2.4	0.00060	1.4	0.0005	23.9	24.0	0.70	6.9	1.7	0.70	5	9.9	2.4	25.4	5.6	0.1410	18.3	4.6
NZ19-7	0.221	1.4	0.306	2.0	0.00010	2.2	0.0002	79.8	79.8	0.72	4.6	3.7	0.68	5	6.8	5.5	23.9	5.0	0.1449	11.6	9.9
NZ19-12*	0.267	1.4	0.291	1.9	0.00008	1.7	0.0010	15.0	15.1	0.91	22.3	3.4	0.61	5	36.3	5.8	45.8	18.6	0.1843		
NZ19-15	0.464	1.3	0.471	1.9	0.00040	1.3	0.0003	32.0	32.0	0.98	4.9	1.6	0.74	5	6.6	2.1	21.4	5.5	0.1983	10.9	3.7
									Weighted mean (in ka BP) ± 95% conf. (in ka) *(MSWD)*:											**11.3 ± 2.6** *(0.54)*	
NZ-20																					
NZ20-17	2.234	1.3	1.857	1.9	0.00052	0.9	0.0016	10.7	10.8	1.19	5.6	0.6	0.74	5	7.6	0.9	77.8	18	0.2399	9.8	1.3
NZ20-16	0.715	1.9	0.725	2.4	0.00016	1.7	0.0007	15.9	16.0	0.98	6.8	1.1	0.72	5	9.4	1.6	145	39	0.1967	10.9	2.0
NZ20-1	0.714	1.3	0.744	2.0	0.00007	2.1	0.0005	35.6	35.7	0.95	4.8	1.7	0.57	10	8.5	3.1	18.4	3.8	0.1913	14.2	5.6
NZ20-3	0.475	1.3	0.516	1.9	0.00017	1.7	0.0004	39.8	39.8	0.91	5.8	2.3	0.65	5	8.9	3.6	32.4	8.2	0.1835	14.0	5.9
NZ20-4	0.677	1.9	0.574	2.4	0.00031	1.3	0.0006	23.0	23.1	1.17	6.5	1.5	0.66	5	9.8	2.3	31	6.8	0.2351	14.9	3.7
NZ20-5	0.459	1.3	0.526	2.0	0.00044	0.7	0.0006	31.6	31.7	0.87	7.1	2.3	0.73	5	9.8	3.2	108	15	0.1741	12.0	4.0
NZ20-7	0.573	1.3	0.672	2.0	0.00020	1.8	0.0004	29.2	29.2	0.85	4.2	1.2	0.68	5	6.2	1.8	19.8	5.2	0.1701	10.9	3.4
NZ20-8	0.507	2.0	0.867	2.4	0.00009	2.1	0.0009	15.7	15.9	0.58	7.2	1.1	0.72	5	10.0	1.7	53.6	11	0.1165	15.9	2.9
									Weighted mean (in ka BP) ± 95% conf. (in ka) *(MSWD)*:											**11.3 ± 1.7** *(0.76)*	

F_t—alpha ejection correction factor calculated after Farley et al. (1996) for homogeneous distribution of parent nuclides; uncertainty on Ft factors was arbitrarily set to 5% and 10% for crystals with Ft ≥ 0.6 and Ft < 0.6, respectively, after Ehlers and Farley (2003) and propagated in quadrature into final age uncertainty; D_{230}—Th zircon-melt fractionation factor calculated after (Farley et al. 2002) using the Th/U ratios of analyzed bulk zircon crystals and whole rock Th/U (NZ-19 = 4.9356; NZ-20 = 4.9793); Diseq.-cor. (U-Th)/He age (ka)—disequilibrium corrected (U-Th)/He age calculated by MCHeCalc program (Schmitt et al. 2010) assuming $D_{231} = 3.3$ (i.e., an average of $f_{Pa/U}$ values published by Schmitt 2007, 2011; Sakata et al. 2017); Eruption ages were calculated as error weighted average by Isoplot 4.15 Excel add-in (Ludwig 2012). Crystal marked with asterisk was disregarded because its (U-Th)/He date is older than the youngest U-Th age. For more details see Supplementary table 1

TAU total analytical uncertainty

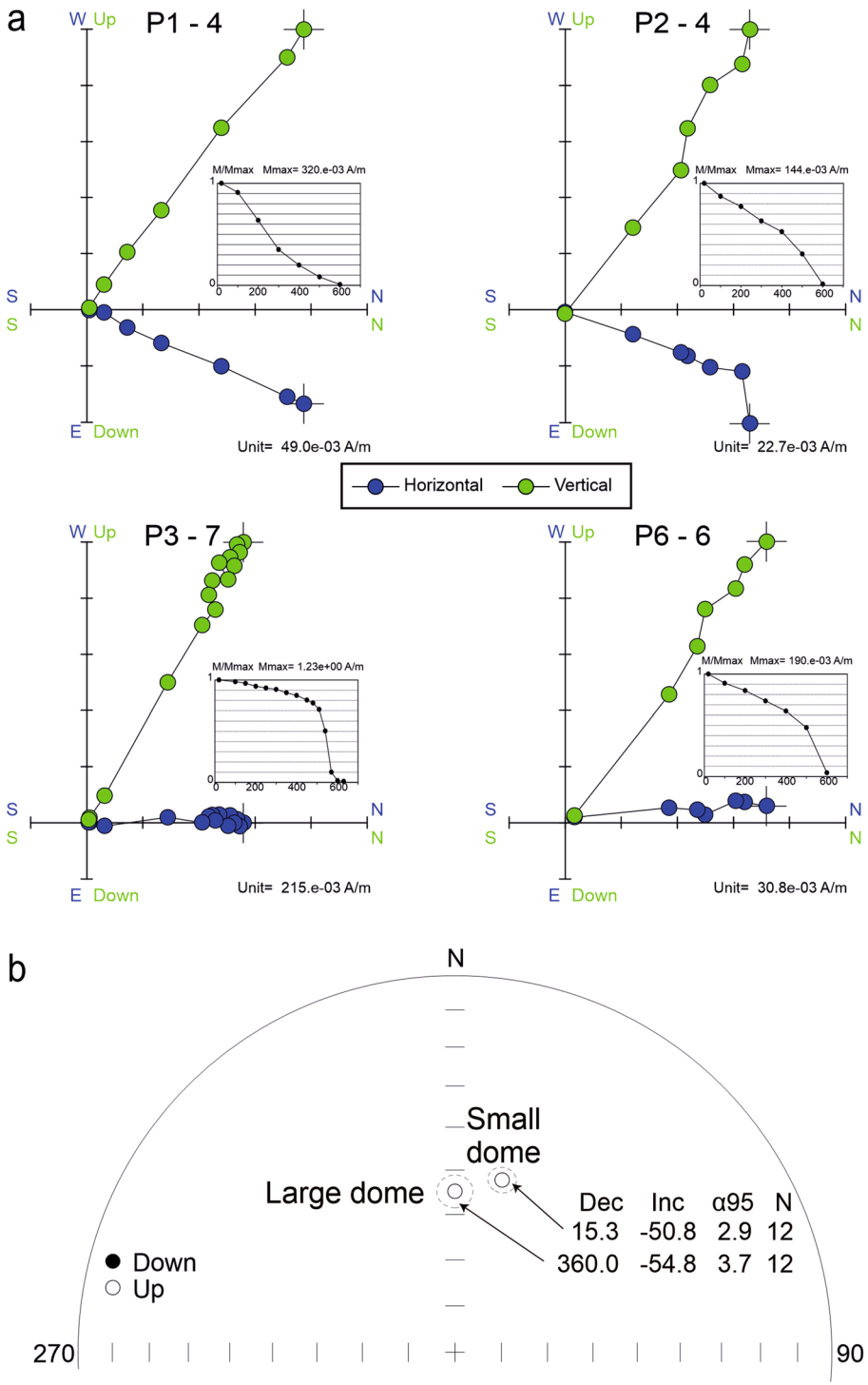

Fig. 5 **a** Representative orthogonal vector plots for NRM obtained during progressive thermal demagnetization with magnetic intensity (M/Mmax) decay curves. Blue and green symbols represent projection onto horizontal and vertical planes, respectively. **b** Equal area projection of characteristic remanent magnetization of samples from large and small domes. Dots (upper hemisphere) indicate mean directions with dashed ovals denoting 95% confidence limits (α95)

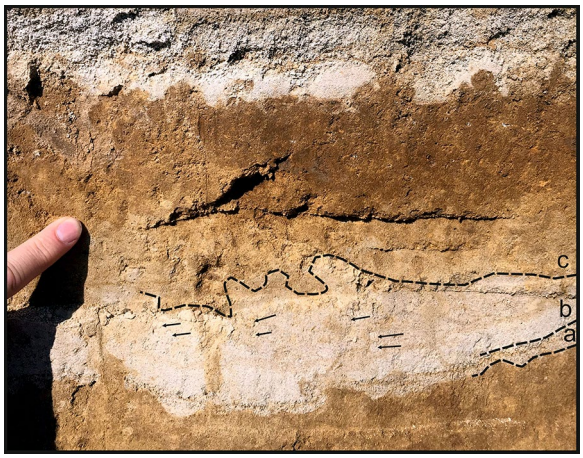

Fig. 6 Close-up view of the newly exposed outcrop of the Puketerata sequence at locality 7–01 (Fig. 1b): **a** pyroclastic fall deposit, **b** PDC origin with accretionary lapilli (arrows), **c** Disturbed ash with PDC origin that transition to a paleosol with high organic matter. A wider shot image of the outcrop is shown in Fig. 7c

emplacements. The angle difference in declination is ca. 15 degrees, whereas the fastest declination change rate calculated from the NZPSV10k curve is 0.18 degree/year (Turner et al. 2015). These results, therefore, suggest at least 83 years as the shortest break between the emplacement of the two lava domes. If the average declination change rate of 0.04 degree/year is applied, it would take 375 years to achieve the measured angle difference. These paleomagnetic dating results disagree with the brief duration of the PVC activity inferred from the volcanic products and architecture as proposed by Brooker et al. (1993) and Kósik et al. (2019). The paleomagnetic results are consistent with a 6–8 cm thick soil horizon at the top of the lower tephra at locality 7–01 (Fig. 6), which we interpret to represent a break in volcanic activity of a few hundred years between phase one and three. This estimate is in line with the soil formation rates of Egli et al. (2018).

We are not able to quantify the time between the maar-forming phase and the emplacement of the small dome (phase 2). Nevertheless, we suggest these two phases likely represent the same eruption period considering the time break between explosive activity that documented at locality 7–01 (Figs. 6 and 7c) and the emplacement of the two domes. Alternatively, it cannot be ruled out that smaller dome represents a separate event.

Revised stratigraphy

The stratigraphical position of Puketerata tephra was established from medial and distal observations (Vucetich and Pullar 1969, 1973). The Puketarata tephra was identified mostly by its biotite content (Topping and Kohn 1973) or exceptionally low TiO_2 and MgO concentrations in glass shards at distal locations (Lowe 1988). However, it was later recognized that Rotorua tephra, sourced from the Okataina Volcanic Centre (Nairn 2002), has biotite and glass compositions remarkably similar to the Puketerata tephra (Shane et al. 2003). Consequently, the compositional similarities identified between Puketerata tephra and Okataina-sourced tephras (e.g., Shane et al. 2003), along with the isopachs and the main direction of the dispersal of Puketerata tephra (Lloyd 1972; Brooker et al. 1993) may discredit the stratigraphic framework of Puketerata tephra that is based on distal locations (D. Lowe, pers. comm. 2022), such as at Lake Rotomanuka (Waikato—37°55′33"S, 175°18′56"E; Lowe 1988). Thus, it can be argued that the currently accepted age of 16 ka for the PVC only relies on an ambiguous stratigraphic correlation.

Vucetich and Pullar (1969) placed the Puketerata tephra between Karapiti and Opepe Tephras of Taupō volcano, bracketing its age between 9.95 and 11.8 ka (Wilson 1993; Lowe et al. 2013). In contrast, Vucetich and Pullar (1973) proposed Rerewhakaaitu Ash (17.6 ka; Darragh et al. 2006) as the lower contact and Rotorua Ash (15.8 ka; Nairn 2002) as the upper contact for the stratigraphic position of Puketerata tephra, and this stratigraphic relationship forms the base for the currently accepted age of ca. 16 ka for Puketerata tephras (e.g., Leonard et al. 2010). It is noteworthy that Vucetich and Pullar (1973) provides no reference to their previous study (Vucetich and Pullar 1969), which, in the light of the new geochronological data presented here, seems to report the correct eruption age.

During the 2016–2017 field survey, more than thirty proximal and medial exposures of Puketerata deposits (Fig. 7) within a 5 km radius from the main Puketerata vent were identified by Kósik et al. (2019). The aim of that study was not to reassess the stratigraphic position of the Puketerata tephra, whereas most of the outcrops are located in an elevated topographic position, where the preservation potential may not be good. Nevertheless, none of these examined exposures contained identifiable tephra layers between the top of the Puketerata deposits and Taupo Pumice Formation, whereas the lower contact at the visited proximal and medial exposures of PVC are solely Maroa-sourced ignimbrites, such as the Orakonui Formation (ca. 256 ka, Leonard 2003) or the 25.4 ka Oruanui Formation and associated reworked deposits (Kósik et al. 2019) (Fig. 7).

The widely accepted stratigraphic position of Puketerata tephra is based on a location near the intersection of Palmer Mill Road and State Highway 1 (Vucetich and Pullar 1973), situated 4 km from the nearest Puketerata vent (Fig. 1b). It is difficult to identify the described

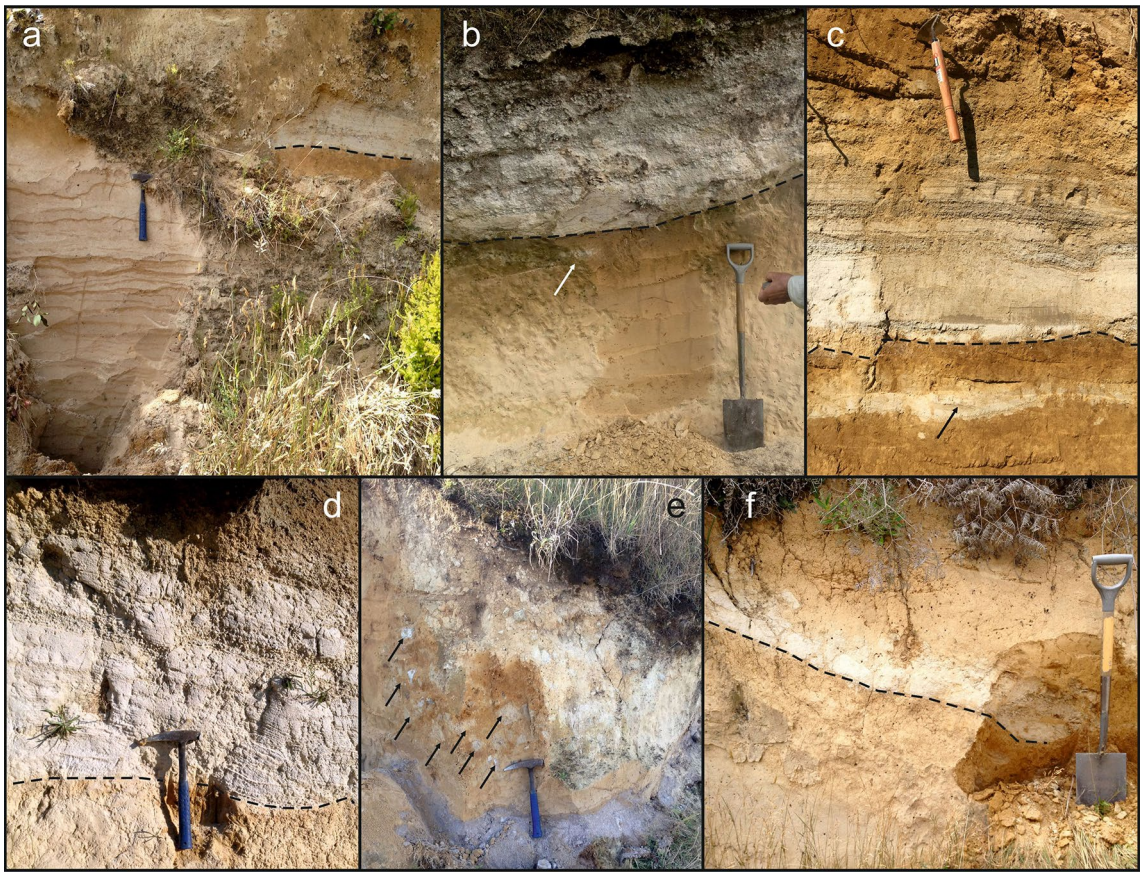

Fig. 7 Representative medial to distal exposures of Puketerata deposits, where black dashed line indicates the base of the main sequence. Black/white arrows most likely refer to deposits of the preceding maar-forming activity. For locations of outcrops refer to Fig. 1b, c. **a** Puketerata sequence at locality 4–17, where Puketerata tephra deposited to a 15 cm thick paleosol that formed on the top of a loess. **b** A patchy layer of fine ash (white arrow) occurs within the 2 m thick paleosol overlain by the main pyroclastic sequence at locality 3–16. The charcoal was collected from the base of the main pyroclastic sequence indicated by black dashed line. **c** The thickest and most continuous fine ash layer that separated by a ca. 10 cm thick paleosol from the main Puketerata deposits at locality 7–01. Arrow indicates the location of the section shown in Fig. 6. **d** Medial Puketerata sequence at locality 4–12. **e** Ignimbrite basement (purplish grey) overlain by floating pieces of unconsolidated Puketerata ash and lithic fragments (black arrows) in reworked paleosol. At the top of the exposure the paleosol also contains 2–3 cm highly vesicular fragments of Taupo Pumice Formation. Note that locality (3–05) represents the rim of a steep wall of a maar crater. **f** Distal exposure of main Puketerata succession at locality 5–18

features on the associated image in the manuscript of Vucetich and Pullar (1973) and the description is rather broad: "12 cm ash (paleosol, dark yellowish brown 19YR 4/4 sandy loam)" on the top and "40 cm pale grey ash and coarse ash; shower-bedded; sharp contact with Rerewhakaaitu Ash below." The outcrop described by Vucetich and Pullar (1973) has not been found during the mapping, whereas other outcrops along Palmer Mill Road expose units in higher stratigraphic positions without the appearance of Puketerata deposits. The stratigraphic position of Puketerata tephra at distal localities has been questioned, as Rotorua tephra has very similar composition and mineral assemblage (Shane et al. 2003). Moreover, the Puketerata tephra is limited in extent (Llyod 1972; Vucetich and Pullar 1973; Brooker et al. 1993) and thus unlikely to crop out south of Lake Taupō (50 km from the vent) or in the Hamilton Basin (100 km from the vent) as published earlier (Topping 1973; Topping and Kohn 1973; Lowe 1988).

The currently accepted age of ca. 16 ka for Puketerata tephra (Vucetich and Pullar 1973; Leonard et al. 2010) is at odds with our new radiometric ages determined by ZDD, ^{14}C dating. This eruption age is in excellent agreement with the age range of 9.95–11.8 ka suggested by Vucetich and Pullar (1969).

As there is no other known silicic eruption in the vicinity of the site since the eruption of the 25.4 ka Oruanui Formation (Leonard et al. 2010), it is likely that the

Puketerata maar—lava dome complex was the source of the lower tephra layer found at locality. 7–01 (Figs. 1 and 6). The sedimentological features of this tephra are consistent with medial deposits that are usually associated with phreatomagmatic activity (Ross et al. 2017; Németh and Kósik 2020).

The lack of diluted PDC-dominated deposits associated with the maar forming phase found in the vicinity of the maar craters was interpreted by a time break in the activity (Kósik et al. 2019). It was suggested that the erosion of tephra associated with the maar forming phase could have been rapid due to the steep slopes and the unconsolidated nature of the tephra, suggesting weeks to months length for the depositional break (Kósik et al. 2019). The new results indicate that the time break instead lasted for centuries, which match much better with the observed poor preservation of the proximal PDC deposits.

Revising the magmatic evolution of Puketerata area and associated hazard implications

The PVC vents are aligned parallel with the Orakeikorako Fault (Lloyd 1972; Kósik et al. 2019), representing a typical example for the interrelation of faulting and volcanic activity of the central TVZ (Kósik et al. 2020; Muirhead et al. 2022). Volcanic evolution of the wider Puketerata area comprises three known eruptions, from which the earliest was basaltic phreatomagmatic activity (Te Hukui; Kósik et al. 2017). Petrography of the basalts from Te Hukui eruption shows interaction between silicic and mafic magma, thus it is feasible that the mafic melt bypassed the silicic magma reservoir, which was the source of the adjacent silicic eruptions of PVC. Mafic recharge of the silicic magma reservoir may trigger renewed zircon crystallization during the ensuing cooling (e.g., Bolhar et al. 2008), thus zircon crystallization ages of Puketerata rocks may overlap with the Te Hukui eruption age. The majority of the Puketerata zircons formed between 50 and 15 ka as evidenced by U-Th disequilibrium data (Wilson and Charlier 2009; this study). Due to the eroded nature of Te Hukui deposits and the absence of material from Oruanui Formation in their deposits (Kósik et al. 2017), we suggest the Te Hukui activity occurred before the 25.4 ka Oruanui supervolcanic eruption.

The first silicic eruption that initially formed the maar craters (phase 1) took place most likely at ca. 12 ka (a few hundred years before the second silicic eruption) based on the stratigraphic relationship at locality 7–01 (Fig. 6). The deposits related to this eruption have rare and often patchy occurrence and more limited dispersal than the following (second silicic) more voluminous eruption. Paleomagnetic data suggest that emplacement of the small dome (phase 2) was part of the first eruption period. The second silicic eruption (phase 3) occurred between 11.3 and 11.7 ka based on ^{14}C and ZDD data, and most likely was triggered by mafic recharge of the magma reservoir (Kósik et al. 2019). The depression of maar craters of the earlier eruptions provided an abundance of groundwater for magma and water interaction. The thick paleosol (Fig. 6) indicates that the climate had ameliorated during the time of both silicic eruptions relative to the preceding colder and dryer conditions.

The magmatic evolution of the Puketerata area indicates that the magma reservoir of Puketerata eruption was active from at least ca. 50 ka as indicated by the range and continuity of zircon crystallization age spectra (Wilson and Charlier 2009; this study) until ca. 12 ka when the last eruptions occurred. It is therefore justified to assume that the Puketerata magma reservoir may still have eruptible melt lenses, particularly as Taupō volcano, located at 30 km to the south, has produced more than 20 eruptions during the Holocene (Barker et al. 2021).

Conclusion

The timing and duration of the activity of the Puketerata maar-lava dome complex (TVZ, New Zealand) was constrained here by three independent dating techniques. Radiocarbon dating of charcoal at the base of the Puketerata sequence yielded age ranges of 11.31–11.65 and 11.66–11.72 cal ka BP at 95.4% probability. Combined $^{238}U/^{230}Th$ disequilibrium and (U-Th)/He dating of zircon from two lava domes indicate eruption ages of 11.3 ± 2.6 ka (large lava dome) and 11.3 ± 1.7 ka (small lava dome). These new results constrain the PVC activity to ca. 11.5 ka, which is significantly younger than the hitherto accepted age of ca. 16 ka determined from earlier stratigraphic observations. Paleomagnetic analysis on the rocks of two lava domes of Puketerata exhibited distinct paleomagnetic directions, suggesting they formed during two separate events at least ca. 100 years apart. Complementary stratigraphic observations are also in agreement with paleomagnetic results and suggest at least a few hundred years quiescence between eruptions. This finding underlines the monogenetic nature of the volcanism where volumetrically minor individual magma batches involved in short lived and small volume eruptions separated by decades produce often compound small volcanoes within a restricted area. Our study highlights that the application of different dating techniques

is important to reveal the timescales of these small-volume eruptions, which is essential to define the hazardscape of volcanic fields.

Abbreviations

MVC	Maroa volcanic centre
PVC	Puketerata volcanic complex
TVZ	Taupō volcanic zone
ZDD	Zircon double-dating

Supplementary Information

The online version contains supplementary material available at https://doi.org/10.1186/s40623-023-01861-0.

Supplementary table 1. Supplementary information for whole rock geochemistry, radiocarbon dating, paleomagnetic analysis and zircon geochronlogy.

Acknowledgements
We thank Harakeke Co Ltd for access to their land. We acknowledge Callum Rees (Massey University) for making useful suggestions on the presentation style. We would like to thank for the constructive reviews of three anonymous reviewers and the manuscript handling and further suggestions by Editor Yuki Yasuda.

Author contributions
SK, TH and MD wrote the manuscript. SK, TH, MD, and NK participated in the field survey and sampling. TH and MO performed all magnetic experiments and measurements and radiocarbon dating. MD, BF and AS carried out the sample preparation and analysis of zircon for geochronology. All authors participated in the interpretation and discussion of the results. All authors read and approved the final manuscript.

Funding
This research was partly supported by JSPS KAKENHI Grant Number JP16K01311, JP16KK0092, JP17K05683 (Takeshi Hasegawa).

Availability of data and materials
The datasets used and/or analyzed during the current study are available as electronic Supplementary table 1 submitted to journal.

Declarations

Ethics approval and consent to participate
Not applicable.

Consent for publication
Not applicable.

Competing interests
The authors declare that the research was conducted in the absence of any commercial or financial relationships that could be construed as a potential competing interests.

Author details
[1]Horizons Regional Council, Private Bag 11025, Palmerston North 4442, New Zealand. [2]Department of Earth Science, Ibaraki University, 2-1-1, Bunkyo, Mito 310-8512, Japan. [3]Western Australia ThermoChronology Facility, John de Laeter Centre, Curtin University, Perth, WA 6845, Australia. [4]Massey University, Private Bag 11-222, Palmerston North 4442, New Zealand. [5]Saudi Geological Survey, Jeddah, Kingdom of Saudi Arabia. [6]Institute of Earth Sciences, Ruprecht-Karls-Universität Heidelberg, Im Neuenheimer Feld 236, 69120 Heidelberg, Germany. [7]Department of Environment and Biodiversity, Paris-Lodron-University of Salzburg, Hellbrunnerstraße 34, 5020 Salzburg, Austria.

Received: 19 August 2022 Accepted: 26 June 2023
Published online: 12 July 2023

References

Acocella V, Spinks KD, Cole JW, Nicol A (2003) Oblique back arc rifting of Taupo Volcanic Zone, New Zealand. Tectonics 22:1045
Barker SJ, Wilson CJN, Illsley-Kemp F, Leonard GS, Mestel ER, Mauriohooho K, Charlier BL (2021) Taupō: an overview of New Zealand's youngest supervolcano. N Z J Geol Geophys 64:320–346
Bolhar R, Weaver SD, Palin JM, Cole JW, Paterson LA (2008) Systematics of zircon crystallisation in the cretaceous separation point suite, New Zealand, using U/Pb isotopes, REE and Ti geothermometry. Contrib Mineral Petrol 156:133–160
Bronk Ramsey C (2017) Methods for summarizing radiocarbon datasets. Radiocarbon 59:1809–1833
Brooker MR, Houghton BF, Wilson CJN, Gamble JA (1993) Pyroclastic phases of a rhyolitic dome-building eruption: Puketarata tuff ring, Taupo Volcanic Zone, New Zealand. Bull Volcanol 55:395–406
Brown SJA, Wilson CJN, Cole JW, Wooden J (1998) The Whakamaru group ignimbrites, Taupo volcanic zone, New Zealand: evidence for reverse tapping of a zoned silicic magmatic system. J Volcanol Geotherm Res 84:1–37
Chako-Tchamabé B, Kereszturi G, Németh K, Carrasco-Núñez G (2016) How polygenetic are monogenetic volcanoes: case studies of some complex maar-diatreme volcanoes. In: Németh K (ed) Updates in volcanology—from volcano modelling to volcano geology 13. IntechOpen, London
Cole JW (1990) Structural control and origin of volcanism in the Taupo volcanic zone, New Zealand. Bull Volcanol 52:445–459
Danišík M, Schmitt AK, Stockli DF, Lovera OM, Dunkl I, Evans NJ (2017) Application of combined U-Th-disequilibrium/U-Pb and (U-Th)/He zircon dating to tephrochronology. Quat Geochronol 40:23–32
Danišík M, Lowe DJ, Schmitt AK, Friedrichs B, Hogg AG, Evans NJ (2020) Submillennial eruptive recurrence in the silicic mangaone subgroup tephra sequence, New Zealand, from bayesian modelling of zircon double-dating and radiocarbon ages. Quat Sci Rev 246:106517
Darragh M, Cole JW, Nairn I, Shane P (2006) Pyroclastic stratigraphy and eruption dynamics of the 21.9 ka Okareka and 17.6 ka Rerewhakaaitu eruption episodes from Tarawera volcano, Okataina volcanic centre, New Zealand. N Z J Geol Geophys 49:309–328
Davey F, Henrys S, Lodolo E (1995) Asymmetric rifting in a continental back-arc environment, North Island, New Zealand. J Volcanol Geotherm Res 68:209–238
Downs DT, Wilson CJN, Cole JW, Rowland JV, Calvert AT, Leonard GS, Keall JM (2014) Age and eruptive center of the Paeroa subgroup ignimbrites (Whakamaru group) within the Taupo Volcanic Zone of New Zealand. Geol Soc Am Bull 126:1131–1144
Egli M, Hunt AG, Dahms D, Raab G, Derungs C, Raimondi S, Yu F (2018) Prediction of soil formation as a function of age using the percolation theory approach. Front Env Sci 6:108
Ehlers TA, Farley KA (2003) Apatite (U–Th)/He thermochronometry: methods and applications to problems in tectonic and surface processes. Earth Planet Sci Lett 206:1–14
Farley KA, Wolf RA, Silver LT (1996) The effects of long alpha-stopping distances on (U-Th)/He ages. Geochim Et Cosmochim Acta 60:4223–4229
Farley KA, Kohn BP, Pillans B (2002) The effects of secular disequilibrium on (U–Th)/He systematics and dating of quaternary volcanic zircon and apatite. Earth Planet Sci Lett 201:117–125
Friedrichs B, Schmitt AK, McGee L, Turner S (2020) U-Th whole rock data and high spatial resolution U-Th disequilibrium and U-Pb zircon ages of Mt. Erciyes and Mt. Hasan quaternary stratovolcanic complexes (Central Anatolia). Data in Brief 29:105113
Fulop A, Kurszlaukis S (2014) It takes two to tango or: how polygenetic is a monogenetic volcano? In: Carrasco-Nunez G, Aranda-Gomez JJ, Ort MH, Silva-Corona JJ (eds) 5th international maar conference abstracts volume. Universidad Nacional Autonoma de Mexico, Centro de Geociencias, Juriquilla
Hogg A, Lowe DJ, Palmer J, Boswijk G, Bronk Ramsey C (2012) Revised calendar date for the Taupo eruption derived by ^{14}C wiggle-matching using a New Zealand kauri ^{14}C calibration data set. Holocene 22:439–449

Hogg A, Heaton TJ, Hua Q, Bayliss A, Blackwell PG, Boswijk G, Bronk Ramsey C, Palmer J, Petchey F, Reimer P et al (2020) SHCAL20 Southern Hemisphere calibration, 0–55,000 years cal BP. Radiocarbon 62:759–778
Kirschvink JL (1980) The least-squares line and plane and the analysis of palaeomagnetic data. Geophys J Roy Astronom Soc 62:699–718
Kósik S, Németh K, Procter JN, Zellmer GF (2017) Maar-diatreme volcanism relating to the pyroclastic sequence of a newly discovered high-alumina basalt in the Maroa Volcanic Centre, Taupo Volcanic Zone, New Zealand. J Volcanol Geotherm Res 341:363–370
Kósik S, Németh K, Lexa J, Procter JN (2019) Understanding the evolution of a small volume silicic fissure eruption: Puketerata volcanic complex, Taupo volcanic zone, New Zealand. J Volcanol Geotherm Res 383:28–46
Kósik S, Bebbington MS, Németh K (2020) Spatio-temporal hazard estimation in the central silicic part of Taupo Volcanic Zone, New Zealand, based on small to medium volume eruptions. Bull Volcanol 82:50
Kósik S, Németh K, Danišík M, Procter JN, Schmitt AK, Friedrichs B, Stewart RB (2021) Shallow subaqueous to emergent intra-caldera silicic volcanism of the Motuoapa Peninsula, Taupo Volcanic Zone, New Zealand–new constraints from geologic mapping, sedimentology and zircon geochronology. J Volcanol Geotherm Res 411:107180
Kósik S, Németh K, Rees C (2022) Integrating LiDAR to unravel the volcanic architecture and eruptive history of the peralkaline Tūhua (Mayor Island) volcano New Zealand. Geomorphology 418:108481
Kurszlaukis S, Fulop A (2013) Factors controlling the internal facies architecture of maar-diatreme volcanoes. Bull Volcanol 75:761
Leonard GS (2003) The evolution of Maroa volcanic centre, Taupo Volcanic Zone. University of Canterbury, Christchurch
Leonard GS, Begg JG, Wilson CJN (2010) Geology of the Rotorua area Institute of Geological and Nuclear Sciences 1:250,000 geological map 5. Sheet + 102 p. GNS Science, Lower Hutt
Lloyd EF (1972) Geology and hot springs of Orakeikorako. New Zeal Geol Surv Bull, New Zealand
Lowe DJ (1988) Stratigraphy, age, composition, and correlation of late quaternary tephras interbedded with organic sediments in Waikato lakes, North Island, New Zealand. N Z J Geol Geophys 31:125–165
Lowe DJ, Blaauw M, Hogg AG, Newnham RM (2013) Ages of 24 widespread tephras erupted since 30,000 years ago in New Zealand, with re-evaluation of the timing and paleoclimatic implications of the Late glacial cool episode recorded at Kaipo bog. Quat Sci Rev 74:170–194
Ludwig KR (2012) User's manual for isoplot 3.75–4.15. Berkeley Geochronology Center
Muirhead JD, Illsley-Kemp F, Barker SJ, Villamor P, Wilson CJN, Otway P, Mestel ERH, Leonard GS, Ellis S, Savage MK, Bannister S, Rowland JV, Townsend D, Hamling IJ, Hreinsdóttir SA, Smith B, McGregor R, Snowden M, Shalla Y (2022) Stretching, shaking, inflating: volcanic-tectonic interactions at a rifting silicic caldera. Front Earth Sci 10:835841
Nairn IA (2002) Geology of the Okataina Volcanic Ventre, scale 1: 50 000. Institute of Geological and Nuclear Sciences, Lower Hutt
Németh K (2010) Monogenetic volcanic fields: origin, sedimentary record, and relationship with polygenetic volcanism. In: Canon-Tapia E, Szakács A (eds) What is a volcano? Geol Soc Am Spec Papers 470:43–66
Németh K, Kereszturi G (2015) Monogenetic volcanism: personal views and discussion. Int J Earth Sci 104:2131–2146
Németh K, Kósik S (2020) Review of explosive hydrovolcanism. Geosciences 10:44
Reiners PW (2005) Zircon (U-Th)/He thermochronometry. Rev Mineral Geochem 58:151–176
Reyners M (2013) The central role of the Hikurangi Plateau in the Cenozoic tectonics of New Zealand and the Southwest Pacific. Earth Planet Sci Lett 361:460–468
Ross P-S, Carrasco-Núñez G, Hayman P (2017) Felsic maar-diatreme volcanoes: a review. Bull Volcanol 79:20
Sakata S, Hirakawa S, Iwano H, Danhara T, Guillong M, Hirata T (2017) A new approach for constraining the magnitude of initial disequilibrium in quaternary zircons by coupled uranium and thorium decay series dating. Quat Geochronol 38:1–12
Schmitt AK (2007) Ion microprobe analysis of (^{231}Pa)/(^{235}U) and an appraisal of protactinium partitioning in igneous zircon. Am Mineral 92:691–694
Schmitt AK (2011) Uranium series accessory crystal dating of magmatic processes. Ann Rev Earth Planet Sci 39:321–349
Schmitt AK, Stockli DF, Hausback BP (2006) Eruption and magma crystallization ages of Las Tres Vírgenes (Baja California) constrained by combined ^{230}Th/^{238}U and (U-Th)/He dating of zircon. J Volcanol Geotherm Res 158:281–295
Schmitt AK, Stockli DF, Niedermann S, Lovera OM, Hausback BP (2010) Eruption ages of Las Tres Vírgenes volcano (Baja California): a tale of two helium isotopes. Quat Geochronol 5:503–511
Schmitt AK, Klitzke M, Gerdes A, Schäfer C (2017) Zircon hafnium–oxygen isotope and trace element petrochronology of intraplate volcanic rocks from the Eifel (Germany) and implications for mantle versus crustal origins of zircon megacrysts. J Petrol 58:1841–1870
Shane PAR, Smith VC, Lowe DJ, Nairn IA (2003) Reidentification of c. 15,700 cal yr BP tephra bed at Kaipo Bog, eastern North Island: implications for dispersal of Rotorua and Puketarata tephra beds. N Z J Geol Geophys 46:591–596
Smith IEM, Németh K (2017) Source to surface model of monogenetic volcanism: a critical review. Geol Soc Lond Spec Publ 446:1–28
Sourisseau D, Macías JL, Tenorio FG, Avellán DR, Girón RS, Bernal JP, Murillo ZT (2020) New insights into the stratigraphy and ^{230}Th/U geochronology of the post-caldera explosive volcanism of La Primavera caldera, Mexico. J South Am Earth Sci 103:102747
Spinks KD, Acocella V, Cole JW, Bassett KN (2005) Structural control of volcanism and caldera development in the transtensional Taupo Volcanic Zone, New Zealand. J Volcanol Geotherm Res 144:7–22
Topping WW (1973) Tephrostratigraphy and chronology of late quaternary eruptives from the Tongariro Volcanic Centre, New Zealand. N Z J Geol Geophys 16:397–423
Topping WW, Kohn BP (1973) Rhyolitic tephra marker beds in the Tongariro area, North Island, New Zealand. N Z J Geol Geophys 16:375–395
Turner GM, Howarth JD, de Gelder GINO, Fitzsimons SJ (2015) A new high-resolution record of Holocene geomagnetic secular variation from New Zealand. Earth Planet Sci Lett 430:296–307
Valentine GA, Gregg TKP (2008) Continental basaltic volcanoes—processes and problems. J Volcanol Geotherm Res 177:857–873
Vucetich CG, Pullar WA (1969) Stratigraphy and chronology of late Pleistocene volcanic ash beds in central North Island, New Zealand. N Z J Geol Geophys 12:784–837
Vucetich CG, Pullar WA (1973) Holocene tephra formations erupted in the Taupo area, and interbedded tephras from other sources. N Z J Geol Geophys 16:745–780
Wallace LM, Beavan J, McCaffrey R, Darby D (2004) Subduction zone coupling and tectonic block rotations in the North Island, New Zealand. J Geophys Res Sol Earth 109:B12406
Wilson CJN (1993) Stratigraphy, chronology, styles and dynamics of late quaternary eruptions from Taupo volcano, New Zealand. Phil Trans R Soc Lond A343:205–306
Wilson CJN, Charlier BLA (2009) Rapid rates of magma generation at contemporaneous magma systems, Taupo volcano, New Zealand: insights from U-Th model-age spectra in zircons. J Petrol 50:875–907
Wilson CJN, Houghton BF, McWilliams MO, Lanphere MA, Weaver SD, Briggs RM (1995) Volcanic and structural evolution of Taupo Volcanic Zone, New Zealand: a review. J Volcanol Geotherm Res 68:1–28

Publisher's Note